AGU PUBLICATIONS

Geophysical Research Letters

Supporting Information for

Pervasive foreshock activity across southern California

Daniel T. Trugman[1], Zachary E. Ross[2]

[1] Geophysics Group, Earth and Environmental Sciences Division, Los Alamos National Laboratory, Los Alamos NM

[2]Seismological Laboratory, California Institute of Technology, Pasadena CA

Corresponding author: Daniel Trugman (dtrugman@lanl.gov)

Contents of this file

Introduction

This supporting information contains Supplementary Text S1, Figures S1-S6, and Supplementary Tables S1 and S2. Text S1 outlines the sensitivity analysis performed for the mainshock selection criteria. Text S2 describes stress change calculations for small magnitude foreshocks. Figure S1 shows a map of spatial variations of the magnitude of completeness in the Quake Template Matching (QTM) catalog. Figure S2 shows the main results of the foreshock analysis using the Southern California Seismic Network (SCSN) catalog instead of the QTM catalog. Figure S3 highlights a foreshock sequence that is missed nearly in its entirety by the SCSN catalog. Figure S4 is analogous to Figure 3 in the main text, provided a pair of foreshock sequences with very different spatiotemporal evolution. Figure S5 shows a spatial map of heat flow for comparison with foreshock prevalence. Figure S6 shows the approximate change in shear stress following M2 and M0 earthquakes. Table S1 lists results of the sensitivity analysis for mainshock selection criteria described in Text S1. Table S2 documents the key features of the 46 mainshocks considered in this study, along with their associated foreshock statistics.

Text S1

This study analyzes foreshock activity preceding mainshock earthquakes with magnitudes M4 and greater within our study region in California. In order to isolate mainshocks where we can examine a clean pre-event window that is uncontaminated by triggered aftershocks of other large earthquakes, we use a magnitude-dependent windowing criterion. Specifically, we exclude all candidate mainshocks that occur within an epicentral distance *R* and time period *T* following another larger earthquake. We parameterize *R* and *T* to increase with the magnitude *M* of the larger earthquake using the following relations:

$$R(M) = R_0 + c_R L(M), \; T(M) = T_0 + c_T (M-4) . \quad (1)$$

Here $L(M)$ is the expected rupture length (Wells & Coppersmith, 1994), $\{R_0, c_r, T_0, c_T\}$ are constants, *R* is measured in days, and *T* is measured in km. The results presented in this study set R_0 = 20 km, $c_r = 5$, T_0 = 50 days, and c_T= 25 days. These choices were designed to be conservative, erring on the side of excluding too many events rather than risking contamination of the foreshock windows with aftershocks of other earthquakes. We performed sensitivity analysis on these parameters, and the key results of our analyses do not vary significantly based on our choice. The results of the sensitivity analysis are presented in Table S1.

Text S2

To get a first-order assessment of the triggering potential of small foreshocks, we calculate the static stress change imposed in an elastic halfspace following slip on a rectangular dislocation (Okada, 1992). We assume an elastic halfspace with 30 GPa shear modulus, and model strike-slip motion on a vertically-oriented, square fault plane (length L = width W) with 3 MPa stress drop. For a range of foreshock magnitudes, we then calculate stress changes along a horizontal slice through the halfspace at the same depth as the source, which we set to 5 km. As shown in Figure S7, for a M2 foreshock, the maximum shear stress, $\tau_{max} = |S_1 - S_3|/2,$ is of order 1 kPa at 500 m distance from the rupture plane (here S_1 and S_3 are principal stresses of the stress change tensor). In contrast, for a M0 earthquake, this same 1kPa contour is located at ~ 50 m distance from the rupture plane. One can show that the radial distance of this contour decreases by a factor of 10 for every 2-unit decrease in magnitude, and hence is located at ~ 5 m distance from the rupture for a M-2 earthquake. While this numerical exercise makes a number of simplifying assumptions and neglects the effects of dynamic stresses, it illustrates that it would be difficult to sustain an extensive sequence of small foreshocks via earthquake-to-earthquake stress triggering alone.

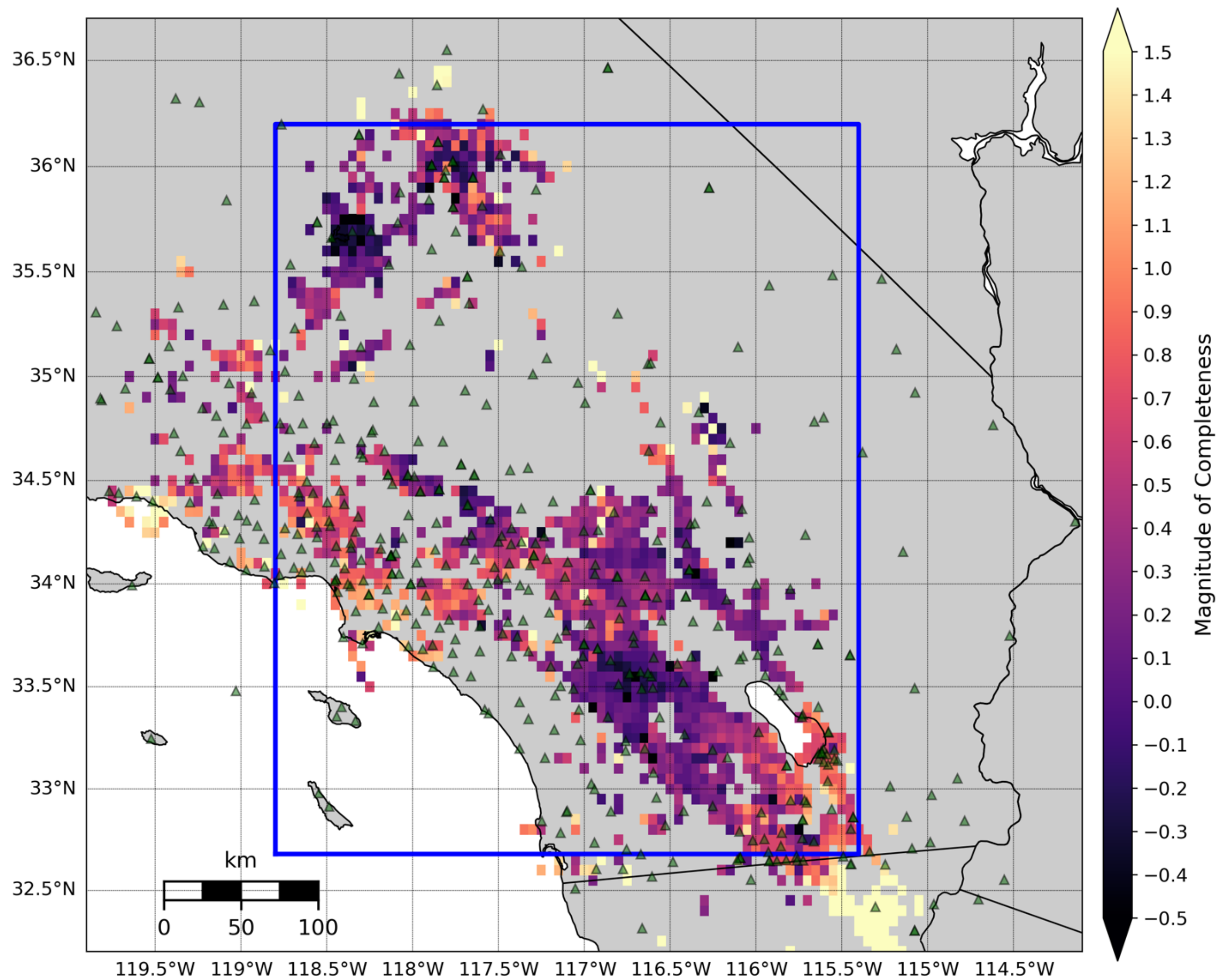

Figure S1. Spatially variable magnitude of completeness, calculated using the goodness-of-fit test (Wiemer & Wyss, 2000) at the 95% confidence level. The study region used in this manuscript is outlined in blue: latitude and longitude ranges of [32.68°, 36.20°] and [-118.80°, -115.40°]. Events are binned with increments of 0.05 degrees in latitude and longitude, and the bins are only plotted if they contain more than 30 events. SCSN stations are marked with green triangles.

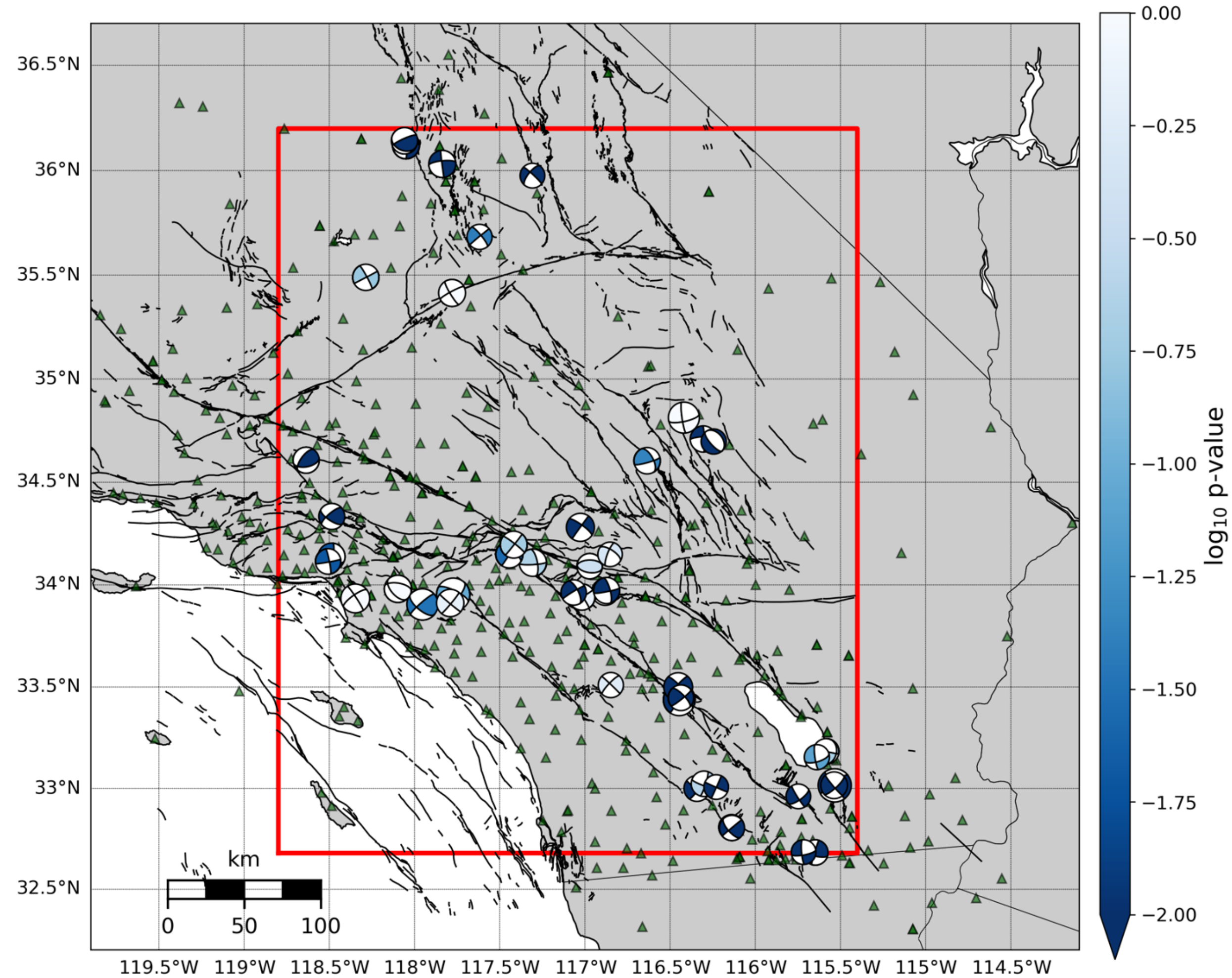

Figure S2. Foreshock sequences of 46 M4 and M5 earthquakes in southern California. Map of 46 mainshocks within our study region that is similar to Figure 1 in the main text, but with the *p*-values computed with the SCSN catalog rather than the QTM catalog. Lower *p*-values (darker colors) indicate more significant activity. In aggregate, the foreshock activity is significantly less well-resolved using the SCSN catalog rather than the QTM catalog.

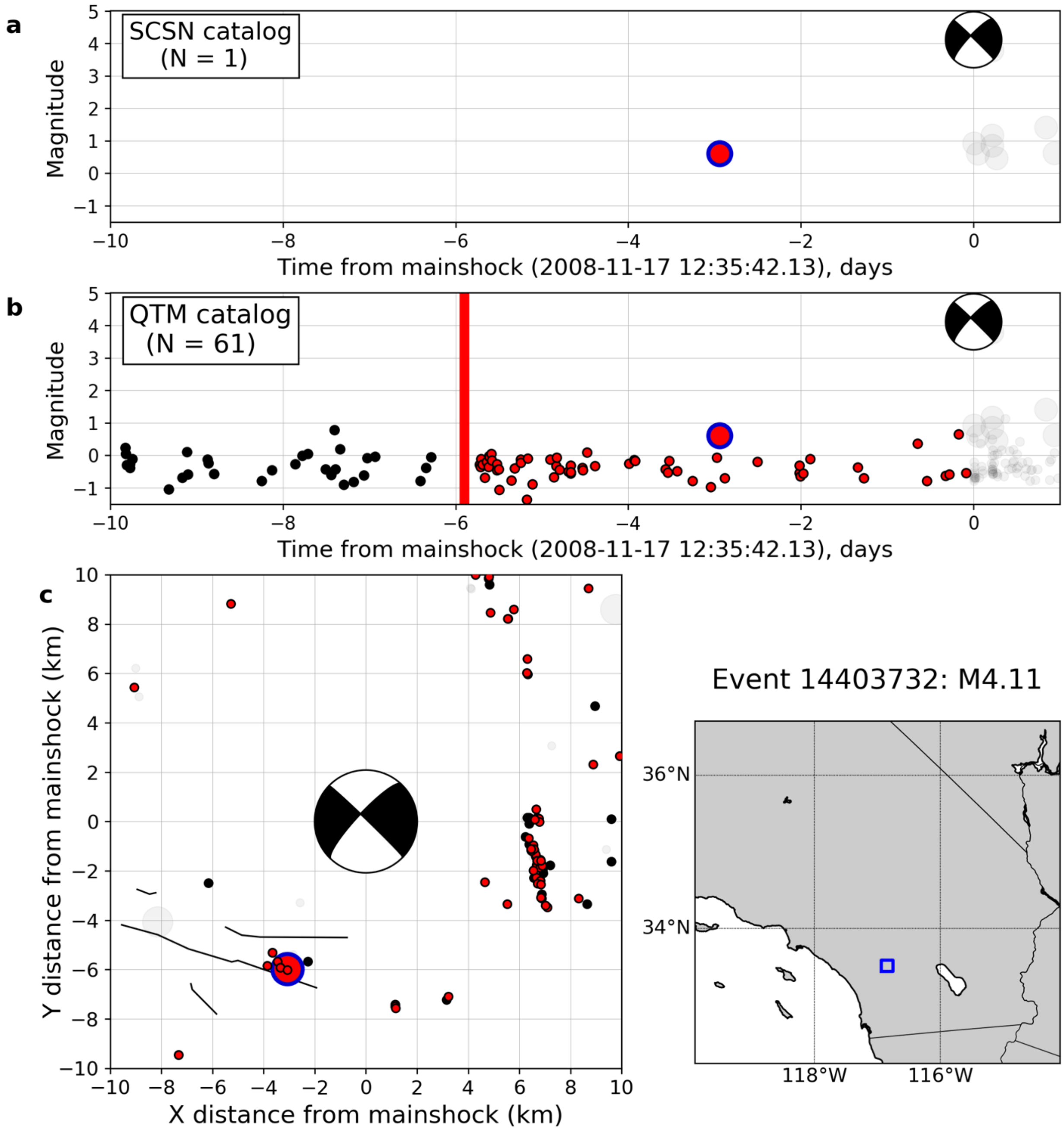

Figure S3. Hidden foreshocks revealed by the improved detection capability of the QTM catalog. Panels (a) and (b) compare the magnitude-time evolution of the foreshock sequence for event 14403732 from the perspective of (a) the SCSN catalog (b) the QTM catalog. In the 6 days preceding this event, only one SCSN earthquake was recorded, compared to 61 in the QTM catalog. Red circles denote events following the estimated foreshock duration (red line), while black circles denote events preceding this. (c) Map view of the foreshock sequence and its location within southern California.

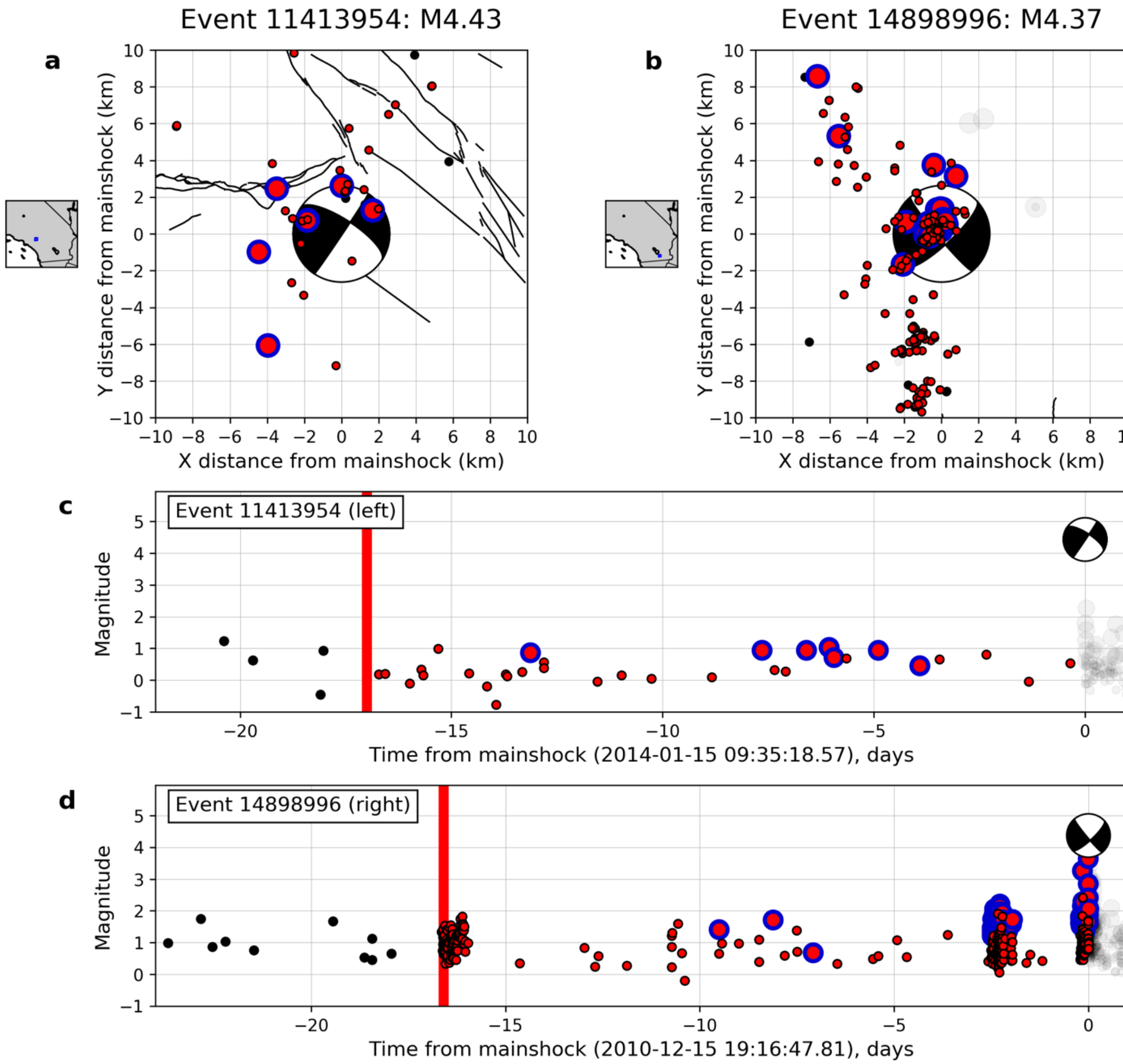

Figure S4. Diverse patterns of foreshock occurrence in southern California. Similar to the Figure 3 in the main text, but with a different contrasting pair of earthquakes. Panels (a) and (b) show map view representations of two distinct foreshock sequences, one (a) with an extended period of elevated seismicity rate surrounding the mainshock hypocenter, and the other (b) with several highly localized bursts of seismicity preceding the mainshock. Red circles denote events following the estimated foreshock duration (red line), while black circles denote events preceding this. Large circles with solid blue lines denote events within the SCSN catalog, while small circles denote newly detected events documented by the QTM catalog. Panels (c) and (d) show magnitude versus time for the sequences shown in panels (a) and (b), respectively. Event 14898996 exhibits migration of foreshock activity toward the eventual mainshock hypocenter, while event 11413954 exhibits a broader activation of foreshock activity with no discernable migration pattern.

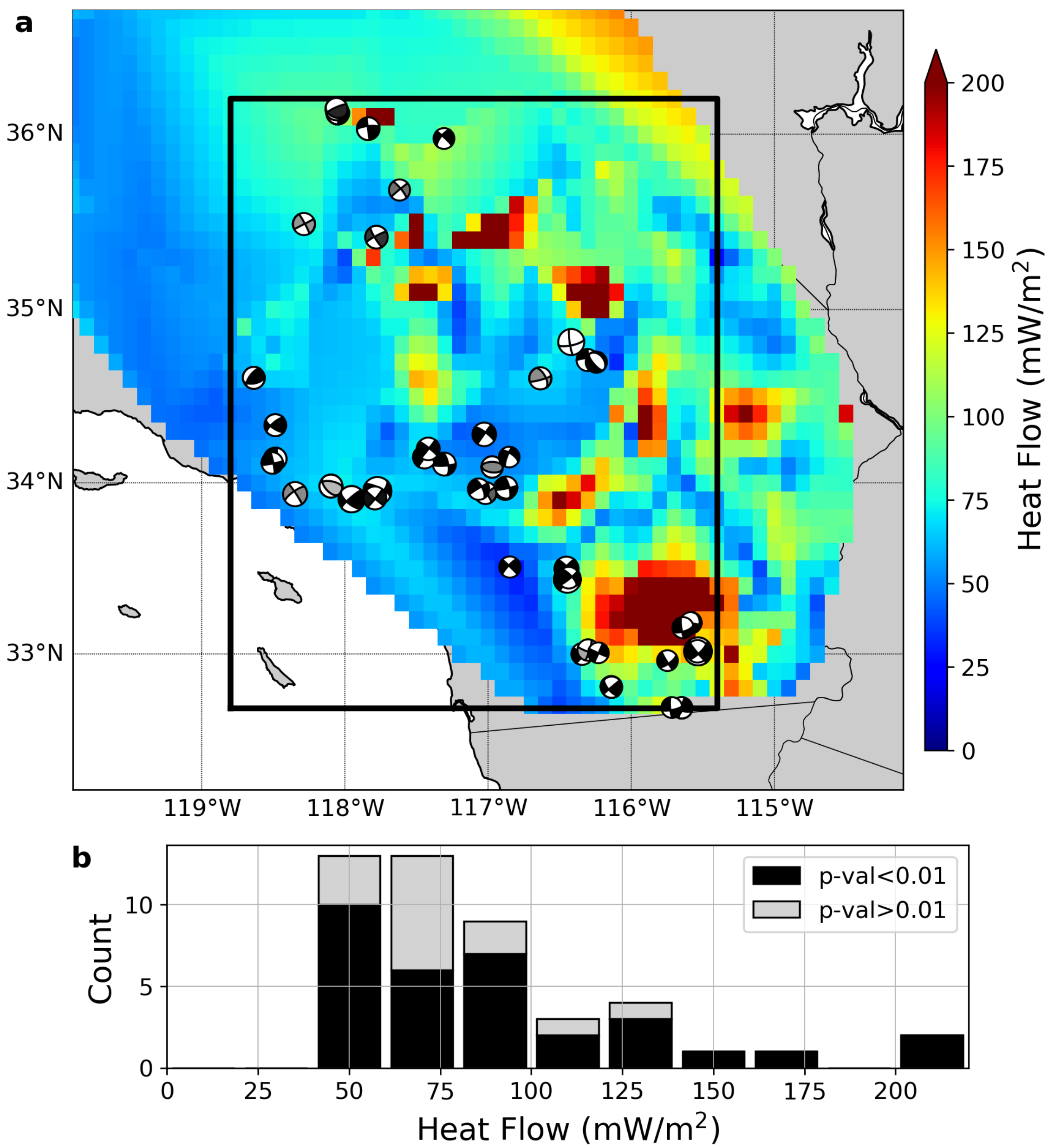

Figure S5. Heat flow map of southern California and relation to foreshock activity. (a) Heat flow data from Blackwell et al. (2011) is linearly interpolated onto a uniform grid with 0.1 degree spacing. Mainshock earthquakes analyzed in this study are marked with their slip mechanisms, with darker colors indicating more significant foreshock activity (lower *p*-values). (b) Heat flow histogram comparison for sequences with *p*-value < 0.01 and > 0.01. The two earthquakes with heat flow values > 200 mW/m^2 are shifted to the rightmost bin in the plot for visual clarity, otherwise they would be off of the listed x-axis scale.

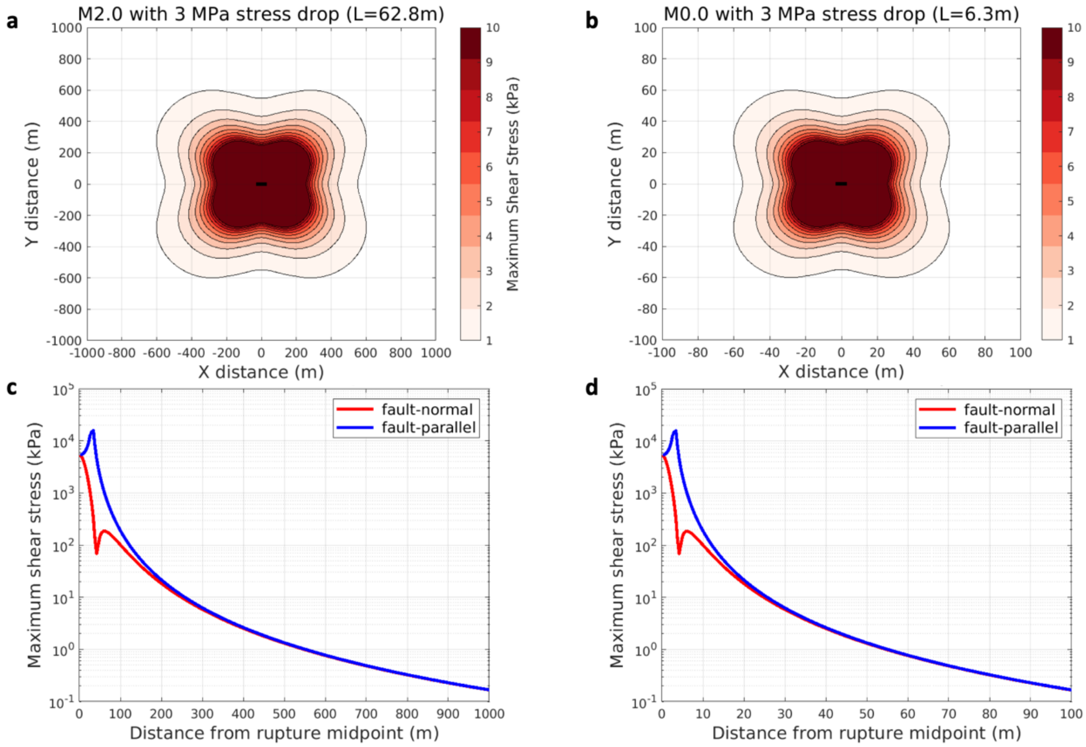

Figure S6. Stress changes from rectangular dislocation in an elastic halfspace (see Text S2). Panels (a) and (b) show a horizontal slice of the calculated maximum change in shear stress for magnitude M2 and M0 earthquakes. The 1 kPa stress contour is located at approximately 500 m and 50 m from the rupture, respectively. Panels (c) and (d) plot the corresponding shear stress changes as a function of distance from the midpoint of the rupture. Note that the panels for the M0 earthquake are identical to those of the M2 earthquake, except the distance axis is rescaled by a factor of 10.

R_0	c_R	T_0	c_T	Number of mainshocks analyzed	Fraction w/ p-value < 0.01: QTM catalog	Fraction w/ p-value < 0.01: SCSN catalog
20	5	50	25	46	33/46 = 72%	22/46 = 48%
20	3	50	25	49	36/49 = 73%	24/49 = 49%
20	7	50	25	46	32/46 = 72%	22/46 = 48%
10	5	50	25	47	34/47 = 72%	23/47 = 49%
30	5	50	25	46	33/46 = 72%	22/46 = 48%
20	5	25	25	48	35/48 = 73%	23/48 = 48%
20	5	75	25	44	31/44 = 70%	21/40 = 53%
20	5	50	15	47	33/47 = 72%	22/47 = 47%
20	5	50	35	46	33/46 = 72%	22/46 = 48%

Table S1. Results of the sensitivity analysis for mainshock isolation criteria (Text S1). The results presented in this study set R_0 = 20 km, $c_r = 5$, T_0 = 50 days, and c_T= 25 days, which is the first row in the table. Each subsequent line perturbs one of these four parameters upwards or downwards from the baseline value in the first row.

Event ID	Origin Time	Latitude (Degrees)	Longitude (Degrees)	Depth (km)	Magnitude	Foreshock *P*-value	Duration (Days)
14383980	2008-07-29 18:42:15	33.95198	-117.77296	16.655	5.44	2.85E-03	-12.4
15200401	2012-08-26 20:57:58	33.01499	-115.53377	8.166	5.41	0.00E+00	-18.1
37374687	2016-06-10 8:04:39	33.43693	-116.4462	12.136	5.19	8.02E-59	-12.2
15481673	2014-03-29 4:09:41	33.90461	-117.95333	6.005	5.09	6.11E-11	-16.6
14408052	2008-12-06 4:18:42	34.81337	-116.41897	7.299	5.06	1.00E+00	NaN
15296281	2013-03-11 16:56:06	33.49917	-116.45238	10.545	4.7	2.86E-21	-10.5
10410337	2009-05-18 3:39:36	33.93396	-118.34765	12.031	4.7	1.19E-01	NaN
15520985	2014-07-05 16:59:34	34.28072	-117.02666	7.257	4.58	3.78E-07	-7.4
15189073	2012-08-08 6:23:34	33.91169	-117.79032	9.266	4.46	1.37E-02	NaN
10370141	2009-01-09 3:49:46	34.10849	-117.30546	15.186	4.45	1.00E-02	-14.6
14601172	2010-03-16 11:04:00	33.98083	-118.09737	18.392	4.44	2.77E-01	NaN
11413954	2014-01-15 9:35:19	34.14917	-117.44353	3.823	4.43	1.66E-05	-17
10527789	2010-01-15 8:23:27	36.0314	-117.83701	2.592	4.41	0.00E+00	-14.6
15476961	2014-03-17 13:25:36	34.13826	-118.48701	9.073	4.4	6.87E-03	-5
37507576	2015-12-30 1:48:57	34.19651	-117.41762	8.329	4.4	2.86E-07	-11.4
15475329	2014-03-13 2:11:04	36.11971	-118.04991	1.769	4.39	3.64E-06	-18.6
37510616	2016-01-06 14:42:35	33.96615	-116.88068	17.066	4.39	1.60E-11	-26.4
14418600	2009-01-31 21:09:22	35.41428	-117.77961	9.945	4.39	2.63E-02	NaN
14898996	2010-12-15 19:16:48	33.01552	-115.53741	7.773	4.37	0.00E+00	-16.6
37526424	2016-02-20 6:13:20	34.60461	-116.63484	9.941	4.31	1.31E-01	NaN

15447161	2013-12-23 13:39:26	36.14198	-118.05878	7.411	4.3	1.98E-02	NaN
11339042	2013-07-24 16:46:02	35.48926	-118.28577	5.581	4.29	1.46E-01	NaN
11373458	2013-10-06 2:06:22	34.70998	-116.30505	10.929	4.28	2.13E-10	-19.6
10530013	2010-01-16 12:03:25	33.94069	-117.01779	15.518	4.28	5.61E-02	NaN
14571828	2010-01-12 2:36:08	33.97258	-116.8724	9.096	4.27	2.10E-18	-15.1
37301704	2015-01-04 3:18:09	34.60709	-118.63591	9.21	4.25	2.02E-33	-29.1
11001205	2011-09-01 20:47:07	34.33383	-118.48573	4.977	4.24	1.30E-20	-15.6
14600292	2010-03-13 16:32:32	32.99978	-116.34234	2.642	4.23	0.00E+00	-23.5
37298672	2014-12-24 5:51:51	33.18247	-115.58426	1.764	4.19	2.28E-24	-17.6
10321561	2008-05-01 3:55:36	33.44677	-116.43617	8.255	4.19	1.15E-35	-34.1
15226257	2012-10-08 0:39:08	33.02293	-116.30118	10.635	4.16	2.08E-01	NaN
15507801	2014-06-02 2:36:43	34.1146	-118.50707	3.045	4.16	1.47E-17	-19.6
11006189	2011-09-14 14:44:51	33.96296	-117.06606	16.525	4.14	4.19E-28	-35.4
14396336	2008-10-02 9:41:49	34.09154	-116.9718	14.984	4.14	1.10E-01	NaN
10489253	2009-11-02 19:27:31	32.68272	-115.64729	6.686	4.13	0.00E+00	-2.8
15223417	2012-10-02 8:28:15	32.80795	-116.1397	9.229	4.13	1.00E+00	NaN
37299263	2016-01-24 15:32:16	34.69768	-116.24407	4.479	4.11	0.00E+00	-31.4
15014900	2011-07-11 1:58:54	32.80423	-116.13689	9.111	4.11	9.00E-15	-28.9
14403732	2008-11-17 12:35:42	33.50928	-116.84783	11.628	4.11	9.53E-04	-5.9
15071220	2011-11-01 15:38:22	35.68315	-117.61833	9.008	4.1	7.26E-02	NaN
37166079	2015-05-21 3:15:30	33.15419	-115.63848	5.831	4.1	8.86E-11	-5.4
14406304	2008-11-30 13:03:07	35.97562	-117.30778	5.596	4.04	0.00E+00	-33.3
37644544	2016-07-31 16:21:05	32.96068	-115.74706	1.113	4.03	7.65E-13	-10.6
15153497	2012-05-22 15:06:24	32.68453	-115.71642	14.447	4.03	4.80E-21	-3.1
15267105	2012-12-22 21:37:45	33.00666	-116.22928	4.576	4.02	1.04E-21	-27.7
37243591	2015-09-16 16:10:47	34.14925	-116.85215	10.706	4	3.49E-05	-4.5

Table S2. Mainshock metadata and foreshock measurements. Foreshock duration is calculated only for sequences with *p*-value < 0.01, and are marked as NaN otherwise.